J Mater Sci: Mater Electron (2008) 19:217–222
DOI 10.1007/s10854-007-9225-5

Pulse plated zinc sulphide films and their characteristics

K. R. Murali · J. Abirami · T. Balasubramanian

Received: 26 January 2007 / Accepted: 22 February 2007 / Published online: 15 March 2007

Abstract Zinc sulphide thin films were deposited by the pulse plating technique using AR grade Zinc sulphate and sodium thiosulphate precursors. The pH of the deposition bath was adjusted to 2. The duty cycle was varied in the range of 20–60%. Total deposition time was kept constant as 60 min in all the cases. X-ray diffraction studies indicated the formation of single phase cubic zinc sulphide films. After heat treatment the crystal structure transformed to hexagonal structure. Optical absorption measurements indicated a band gap values in the range of 3.6–4.0 eV as the duty cycle decreased. EDAX studies yielded a composition of the films deposited at 50% duty cycle is Zn = 48%, S = 52%. XPS studies indicated the formation of ZnS. The Zn 2p and S 3p peaks are observed. AFM studies indicated a rms value of surface roughness of 55 nm for the films deposited at a duty cycle of 60%.

Keywords ZnS fims · II–VI · Pulse plating · Properties

1 Introduction

Zinc sulfide is a wide-band-gap semiconductor with a range of potential applications in optoelectronic devices. It is an excellent host material for electroluminescent phosphors and is being commercially used for electroluminescent displays. Thin films of ZnS doped with rare-earth ions have been extensively studied in view to achieve multi-colour emission [1–3]. ZnS:Mn and ZnMgS:Mn are some interesting phos-phors for the electroluminescent displays [4, 5]. ZnS is also used as n-type window layer for thin-film heterojunction solar cells. ZnS/Cu(In,Ga)Se2 photovoltaic cells have shown an efficiency of 17.2% [6]. ZnS thin films have been prepared by a variety of techniques: thermal evaporation [4], electron beam evaporation, sputtering [7], spray pyrolysis [8], and recently by high-temperature growth onto silicon substrates by pulsed laser deposition [9]. In this investigation, ZnS films have been deposited by the pulse plating technique. Though there exist an earlier work on pulse deposited ZnS films, only duty cycles greater than 50% was used and the concentration of the precursors was varied [10]. In this work, the films were deposited at different duty cycles in the range of 20–60%. To our knowledge this is the first report on ZnS films pulse deposited at different duty cycles.

2 Experimental methods

ZnS films were deposited by the pulse plating technique at different duty cycles in the range 0f 20–60%. The substrates used were conducting glass and titanium. The substrates were cleaned prior to deposition. Titanium substrates were etched in HF solution for a short period and then washed thoroughly to remove traces of acid. The conducting glass substrates were dipped in dilute HCl for about ten minutes and then washed thoroughly to remove traces of acid. Both substrates were finally washed with trichloroethylene and then kept in a dessicator prior to deposition. The deposition precursors were AR grade Zinc sulphate and sodium thiosulphate. About 20 ml of 0.25 M

K. R. Murali (✉)
Electrochemical Materials Science Division, Central Electrochemical Research Institute, CECRI Campus, Karaikudi, Tamilnadu 630 006, India
e-mail: muraliramkrish@gmail.com

J. Abirami · T. Balasubramanian
Deptartment of Physics, Kongunadu Arts and Science College, Coimbatore, Tamilnadu, India

zinc sulphate and 15 ml of 0.30 M sodium thiosulphate were used. The cleaned substrates were used as the cathode and graphite was used as anode. Using SCE as the reference electrode, the potential was fixed as –0.9 V by means of a microprocessor based pulse plating unit. The duty cycle was varied in the range of 20–60%. The deposition temperature was maintained as room temperature. The total deposition time was kept constant as 60 min in all the cases. The thickness of the films was estimated by the weight difference method. All the substrates were weighed using a Mettler semimicro balance prior to deposition. The weight of the substrate after deposition was also measured. Using the density value of bulk ZnS, the thickness was computed. The thickness of the film varies in the range of 1.5–2.5 micrometres as the duty cycle increased. The as deposited films were heat treated in argon atmosphere for a period of 15 min at different temperatures in the range 450–550 °C. Heat treatment was performed to increase the photoactivity of the films. The films were characterized by X-ray diffraction studies using PANalytical X-ray diffractometer and CuKα radiation. Optical absorption studies were made on the films using UV–VIS–NIR Hitachi U3400 spectrophotometer. XPS studies were made using VG MKIII spectrometer and MgKα radiation. EDAX studies were made in a JOEL SEM attached with EDAX set up. AFM studies were made by Molecular Imaging system. For electrical measurements, Indium dot was evaporated on the top surface of the film and the cross plane resistivity was measured by the two probe resistivity method.

3 Results and discussion

The as deposited as well as the post heat treated films were characterized by X-ray diffraction studies. Figure 1 shows the XRD patterns of the ZnS films deposited at different duty cycles. The films exhibit broad XRD patterns indicating the formation of nanocrystalline ZnS films. The peaks corresponding to the cubic phase with (111), (220) and (311) reflections. The crystallite size was computed using the built in software of the XRD unit. The crystallite size is found to vary in the range of 20–45 nm as the duty cycle increases. This is understandable, since, at lower duty cycles, the flux of ions available for deposition at the cathode is only for a short time. For the films deposited at higher duty cycles the flux of ions are available for a longer time for deposition at the cathode, hence the crystallite size is larger for the films deposited at higher duty cycles. The experimental XRD data coincide with the JCPDS data for ZnS cubuc system. The films were post heat treated at different temperatures in the range 450–550 °C in argon atmosphere in order to induce photoactivity in the films. Figure 2 exhibits the XRD pattern of the post annealed

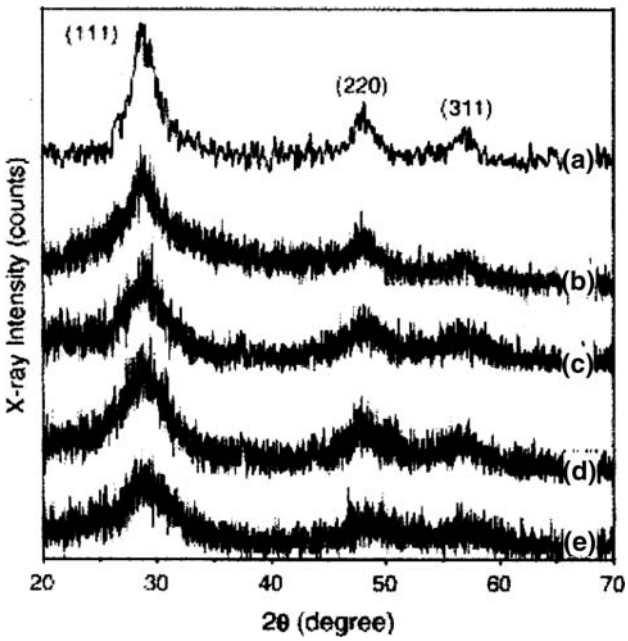

Fig. 1 X-ray Diffraction pattern of the ZnS films deposited at different duty cycles (**a**) 60% (**b**) 50% (**c**) 40% (**d**) 30% (**e**) 20%

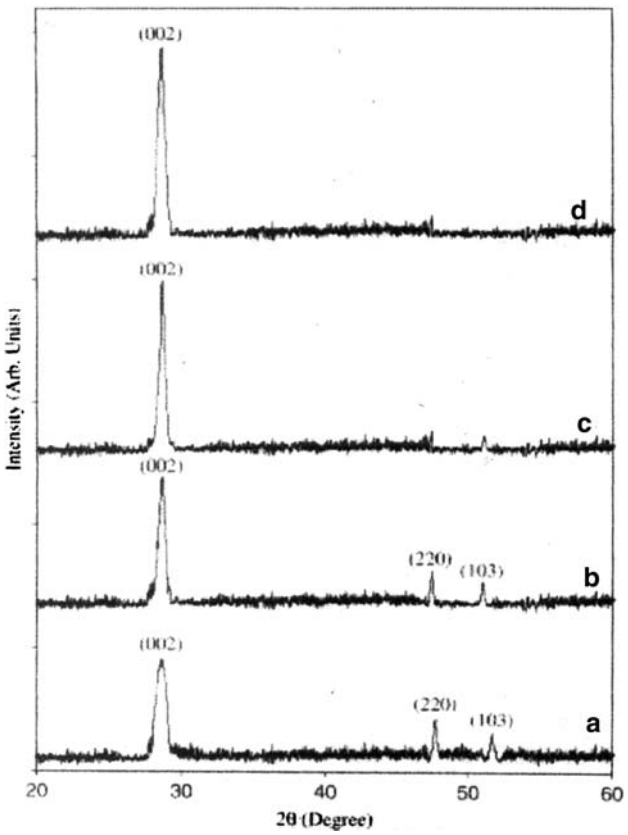

Fig. 2 X-ray diffraction pattern of the ZnS films deposited at 50% duty cycle and post annealed in argon at different temperatures (**a**) 450 °C (**b**) 500 °C (**c**) 525 °C (**d**) 550 °C

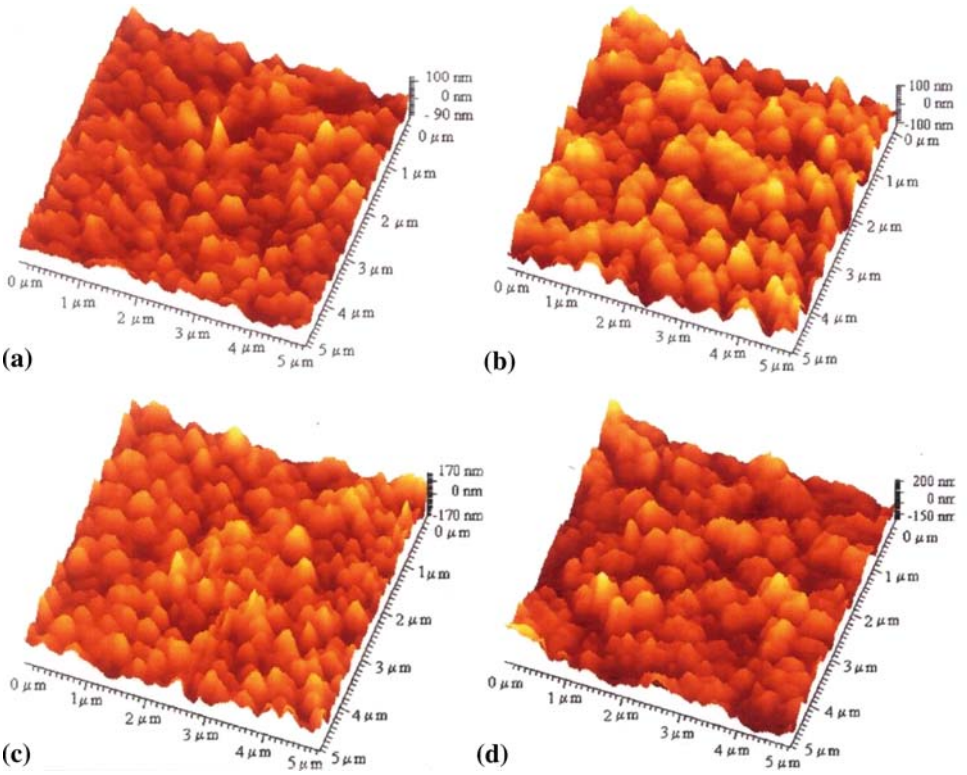

Fig. 3 Atomic Force Micrographs of ZnS films deposited at different duty cycles (**a**) 20% (**b**) 40% (**c**) 50% (**d**) 60%

films deposited at a duty cycle of 50%. It is observed that the crystal structure changes from the cubic to the hexagonal phase as the heat treatment temperature increases from 450 to 550 °C.

For the films heated at 450 °C, two peaks corresponding to hexagonal ZnS and one small peak corresponding to (220) reflection of the cubic phase was observed. As the temperature of heat treatment increases, this peak disappears and the hexagonal peak at (002) reflection was observed to increase in intensity indicating this to be the preferential orientation. Finally for the films deposited at 550 °C only the (002) peak was observed. The width of the XRD patterns were found to decrease in all cases after heat treatment, indicating the increase in crystallite size after heat treatment. Surface morphology of the films was studied using a Molecular Imaging Atomic Force Microscope. Figure 3 shows the AFM micrographs of the films deposited at different duty cycles. The microstructural features of these films are characterized by high-density columnar structure with low surface roughness. One can observe that by increasing the duty cycle from 20 to 60%, the grains of the deposited films are getting larger and begin to agglomerate and coalesce. The roughness parameters obtained in this study are presented in Table 1. The average roughness (Ra) increase from 21.1 to 48.3 nm and the root mean square roughness (Rq) increase from 28.2 to 55.7 nm when the duty cycle increases from 20 to 60%. X-ray photoelectron spectroscopy studies were made on the films deposited at different duty cycles. A standard X-ray source of 15 kV, 300 W and MgKα(1253.6) was used. Figure 4 shows such a spectrum. The signals corresponding to Zn2p3/2 and S2p are observed in all cases. As the duty cycle increases the area under the curves slightly increases. The Zn2p3/2 and S2p signals are observed at Binding energies of 1021.99 eV (Fig. 4a) and 161.44 eV (Fig. 4b) respectively. The curves are Guassian. The value of the composition estimated from this data is 1:1 (Zn:S). These values are agreeing well with the literature value. The atomic concentrations were determined from the peak areas using the Shirley [11] background subtraction, and sensitivity factors provided by the spectrometer manufacturer. Energy dispersive analysis of X-rays (EDAX) showed the presence of zinc and sulphur, with sulphur present slightly more than the stoichiometric ratio. The imbalance may be due to the slight excess of Sulphur deposition. Figure 5 shows the EDAX spectrum of the ZnS films deposited at a duty cycle of 50%. The composition of the films deposited at 50% duty cycle is Zn = 48%, S = 52%. Optical absorption measurements were made at room temperature using unpolarized radiation. Absorbance spectra of the films were recorded as a function of wavelength in the range 250–800 nm. The substrate absorption, if any was corrected by introducing an uncoated clean conducting glass substrate of the same size in the reference beam. Absorption coefficient(α) at various wavelengths was calculated using the Eq. [12].

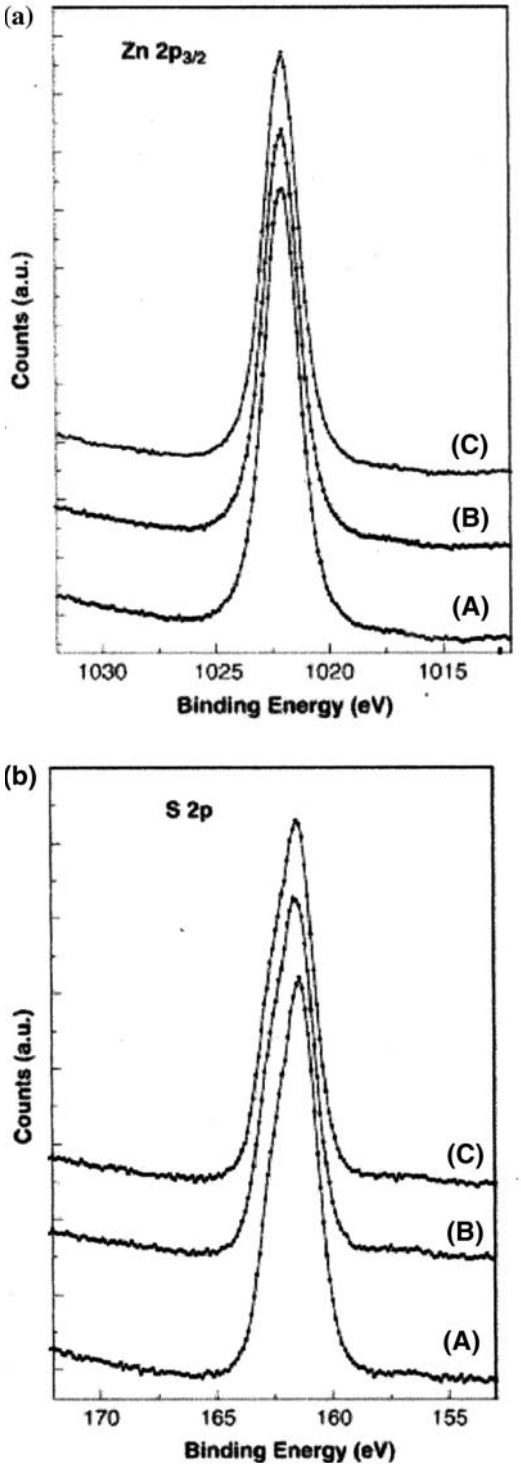

Fig. 4 (**a**) XPS spectrum of Zn in ZnS films deposited at different duty cycles (**A**) 20% (**B**) 40% (**C**) 60%. (**b**) XPS spectrum of S in ZnS films deposited at different duty cycles (**A**) 20% (**B**) 40% (**C**) 60%

$$\alpha = 2.303A/t$$

Where 'A' is the absorbance value at a particular wavelength and 't' is the thickness of the semiconductor film.

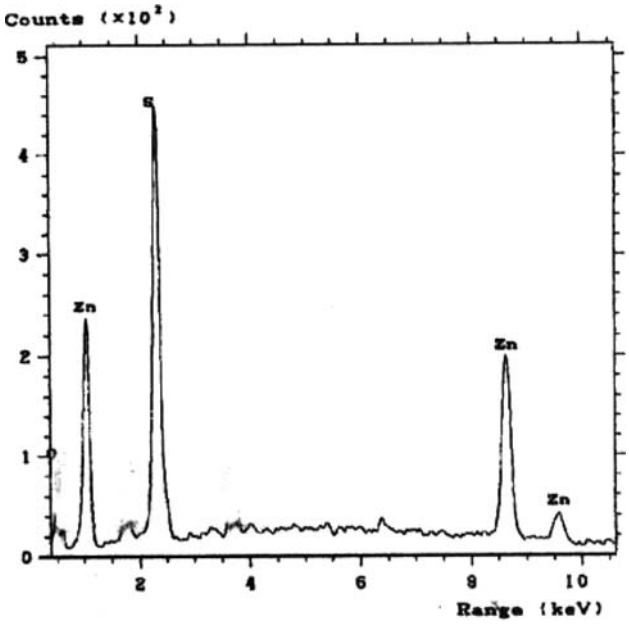

Fig. 5 EDAX analysis of the ZnS film deposited at 50% duty cycle

The band gap of the films was determined by plotting a graph between (αhν)2 versus hν. Extrapolation of the straight line to the hν axis gives the band gap of the film. Figure 6 shows the plot of (αhν)2 versus hν for the films deposited at different duty cycles. The absorption coefficient(α) was found to be of the order of 10^4 cm^{-1}. It can be observed from the figure that the band gap increases with decrease of duty cycle. This is understandable since, the films deposited at lower duty cycle possess a smaller crystal size compared to the films deposited at higher duty

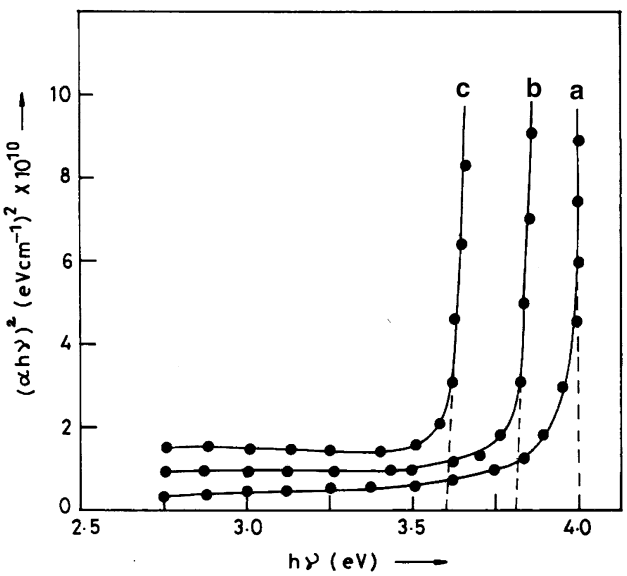

Fig. 6 $(\alpha h\nu)^2$ versus hν plot of ZnS films deposited at different duty cycles (**a**) 20% (**b**) 40% (**c**) 60%

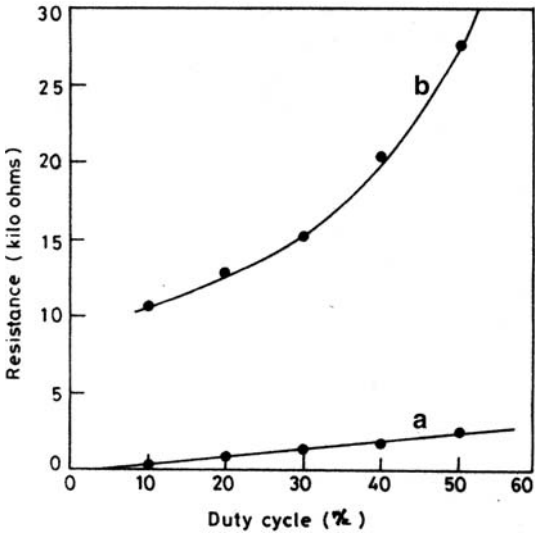

Fig. 7 Variation of resistance with duty cycle(**a**) films heat treated at 550 °C (**b**) as deposited films

cycle. Hence, the larger band gap values are due to quantum size effects. These values are similar to the values reported earlier [13,14]. Electrical resistivity measurements were made on the as deposited as well as heat treated films and deposited at different duty cycles. Indium was deposited on the top of the films and the in plane resistivity of the films were measured using two probe technique. Figure 7 shows the variation of resistivity with duty cycle. The as deposited films were highly resistive in nature with resistivity values increasing as the duty cycle increased. The resistivity decreased after the films were heat treated at a temperature of 550 °C in argon atmosphere. This is due to

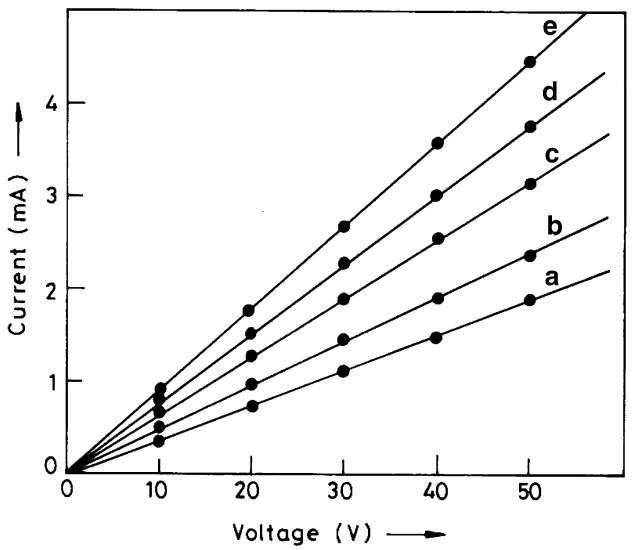

Fig. 8 I–V characteristics of the ZnS films deposited at different duty cycles (**a**) 20% (**b**) 30% (**c**) 40% (**d**) 50% (**e**) 60%

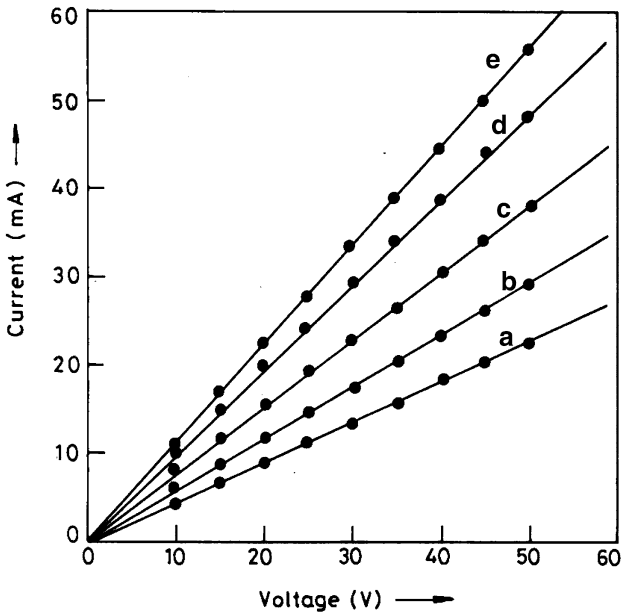

Fig. 9 I–V characteristics of ZnS films deposited at 50% duty cycle and post heat treated at different temperatures (**a**) 450 °C (**b**)475 °C (**c**) 500 °C (**d**) 525 °C (**e**) 550 °C

the fact that the stoichiometry of the films slightly changed after heat treatment. Generally the chalcogen vacancies are responsible for the conductivity in II–VI compounds. The resistivity values are lower than the chemically deposited ZnS films. The conduction mechanism in semiconductors can be understood by analyzing the current–voltage(I–V) plots. For single carrier injection at low voltages, the plot is generally a straight line showing the validity of Ohm's law. I–V characteristics of the as deposited films is shown in Fig. 8. The voltage was applied by using a DC power supply APLAB model high voltage power supply. The applied voltage was varied from 0 to 50 V. The current was measured using a Keithley digital multimeter. The plots are all linear. Figure 9 shows the current–voltage characteristics of the annealed films. The current flowing through the films increased due to the decrease of resistance of the films on annealing. This linear behaviour is attributed to the filling of a discrete set of traps lying at or below the Fermi level. The applied voltage could not be increased beyond 50 V since the films got punctured.

4 Conclusion

The results of this investigation indicate that ZnS films for solar cell applications can be easily deposited by the pulse plating technique. Nanosized crystallites can be obtained. The band gap can be varied by decreasing the crystallite size. The resistance of the films can be further decreased by

doping with impurities. Further work is in progress for obtaining luminescence from these films by doping with Mn and Cu.

References

1. S. Takata, T. Minami, T. Miyata, Thin solid films **193**, 481 (1990)
2. R. Boyn, Phys. Stat. Sol(b) **148**, 11 (1998)
3. G. Harkeman, M. Leppanen, E. Scilinen, R. Ionopist, I. Vijanen, J. Alloy. Comp **225**, 134 (1995)
4. V. Dimilova, J. Tate, Thin solid films **365**, 134 (2000)
5. M.K. Jayaraj, A. Antony, P. Deneshan, Thin solid films **389**, 284 (2001)
6. T. Nakada, M. Mizutani, Y. Hagiwara, A. Kunishka, Solar Energ Mater, Sol. Cells **67**, 255 (2001)
7. L.J. Shan, K.H. Chang, H.L. Hwang, Appl. Surf. Sci. **212**, 305 (2003)
8. N. Tohge, S. Tanaka, K. Okayama, Jpn. J. Appl. Phys. **34**, L207 (1995)
9. Y.Z. Yoo, M. Kawasaki, H. Koinama et al., Appl. Phys. Lett. **78**, 616 (2001)
10. T. Ben Nasr, N. Kamoun, C. Guasch, Mater. Chem. Phys. **96**, 84 (2005)
11. D.A. Shirley, Phys. Rev. **B5**, 4709 (1972)
12. T.H. Yeh, A.E. Blakeslee, J. Electrochem. Soc. **110**, 1018 (1963)
13. J.M. Dona, J. Herrero, J. Electrochem. Soc. **141**, 205 (1994)
14. Ran Zhai, Shubo Wang, Hai Yan Xu, Hao Wang, Hui Yan, Mater. Lett. 59, 1497 (2005)